Structural Engineering and Mechanics, *Vol. 75, No. 6 (2020) 685-699*
DOI: https://doi.org/10.12989/sem.2020.75.6.685

Polygonal finite element modeling of crack propagation via automatic adaptive mesh refinement

M. Shahrezaei and H. Moslemi*

Department of Civil Engineering, Shahed University, Persian Gulf Highway, Tehran, Iran

(Received March 19, 2020, Revised August 5, 2020, Accepted August 6, 2020)

Abstract. Polygonal finite element provides a great flexibility in mesh generation of crack propagation problems where the topology of the domain changes significantly. However, the control of the discretization error in such problems is a main concern. In this paper, a polygonal-FEM is presented in modeling of crack propagation problems via an automatic adaptive mesh refinement procedure. The adaptive mesh refinement is accomplished based on the Zienkiewicz–Zhu error estimator in conjunction with a weighted SPR technique. Adaptive mesh refinement is employed in some steps for reduction of the discretization error and not for tracking the crack. In the steps that no adaptive mesh refinement is required, local modifications are applied on the mesh to prevent poor polygonal element shapes. Finally, several numerical examples are analyzed to demonstrate the efficiency, accuracy and robustness of the proposed computational algorithm in crack propagation problems.

Keywords: polygonal finite element; adaptive mesh refinement; error estimation; crack propagation; linear fracture mechanics

1. Introduction

To predict the fracture and failure of structural components, the behavior of existing cracks in the structure should be investigated. Over the last decades, extensive theoretical and applied studies have dealt with the simulation of the failure mechanism in materials. Although numerical difficulties still exist, the finite element method provides an approach to predict the failure behavior of materials. The main challenge of modeling the crack propagation using FEM is the proper modeling of strong discontinuities in displacements caused by the growth of crack. After the pioneering work of Griffith (1921) on brittle fracture of glass, various alternative approaches have been proposed to simulate the behavior of cracked structures more realistic. Ingraffea (2004) has represented a thorough survey of the computational methods in fracture mechanics while comparing their abilities. The most common methods generally require step-by-step complete remeshing of the global model. However, this procedure is computationally expensive and some alternative methods have been proposed to model the crack growth without remeshing (Moës *et al*. 1999, Sukumar *et al*. 2000, Zi *et al*. 2007).

Polygonal finite element method has been recently employed in modeling of crack propagation. The advantages of this method include greater flexibility in the meshing of arbitrary geometries, better accuracy in the numerical solution because of their higher order shape functions, and no requirement for overall remeshing in crack growth which is inevitable in classic triangular and quadrilateral elements. The idea of polygonal FEM dates back to 1975 when Wachspress (1975) used barycentric coordinates and rational basis for shape functions. However, there is no unique way for construction of the shape functions over the polygon elements and several approaches were proposed by researchers including modified polynomial rational functions (Meyer *et al*. 2002), natural neighbor based coordinates (Sibson 1980), mean value theorem for harmonic functions (Floater 2003) and geometrical properties of the element (Malsch *et al*. 2005). Warren (1996) extended the standard barycentric coordinate functions for simplices to arbitrary convex polytopes combining the adjoints of various dual cones associated with the polytope. Sukumar (2004) employed the maximum entropy principle to construct the polygonal interpolants for convex and concave polygons. Dasgupta (2003) proposed an integration algorithm for polygonal and polyhedral domains using divergence theorem. An efficient methodology for automatic dynamic crack propagation simulations using polygon elements was developed by Ooi *et al*. (2013) based on the scaled boundary finite element method (SBFEM). They accommodated crack propagation via an automatic local remeshing algorithm involving only a small patch of polygons around the crack tip. Talischi *et al*. (2012) presented a simple and robust code for polygonal mesh generation based on the centroidal Voronoi diagrams.

Virtual element method (VEM) was introduced by Beirão Da Veiga *et al*. (2013) for complicated element geometries and higher-order continuity conditions with the addition of suitable non-polynomial functions. They take the spaces and the degrees of freedom in such a way that the elementary stiffness matrix can be computed without actually computing these non-polynomial functions, but just

∗Corresponding author, Ph.D.
E-mail: h.moslemi@shahed.ac.ir

ISSN: 1225-4568 (Print), 1598-6217 (Online)

using the degrees of freedom. Hussein *et al*. (2019) applied VEM to crack-propagation in elastic solids for meshes with highly irregular shaped elements and arbitrary number of nodes. They developed the robust cutting techniques through elements for crack propagation in two dimensional solids using VEM. Leon *et al*. (2014) employed polygonal finite element in dynamic fracture simulations to reduce mesh bias. They proposed an adaptive element splitting algorithm to increase the number of potential crack directions. Spring *et al*. (2014) proposed a scheme for adaptive mesh refinement on unstructured polygonal meshes to better capture crack patterns in dynamic cohesive fracture simulations. This scheme was selectively chosen to optimize the number of paths that a crack may travel, while still maintaining a conforming domain discretization. A polygonal FEM was presented by Khoei *et al*. (2015) for crack growth simulation with minimum remeshing. They modified the convex and concave polygonal elements based on the singular quarter point isoparametric concept to improve the accuracy of the stress intensity factors. A Voronoi polygonal hybrid finite elements with boundary integrals was developed by Wang and Qin (2017). They converted element domain integral in the two-field functional into element boundary integrals to reduce integration dimension. Hoshina *et al*. (2018) proposed a new computational strategy for adaptive local mesh refinement using polygonal finite elements in arbitrary two-dimensional domains. They performed a mesh refinement in regions of material concentration, and a mesh derefinement in regions of low material concentration. An extended polygonal finite element method was presented by Hyunh *et al*. (2019) for large deformation fracture analysis. They used a polygonal mesh to represent space of the present numerical technique in advance, and then a local refinement of structured meshes at the vicinity of the discontinuities is additionally established.

One of the challenging problems in numerical solutions of crack propagation problems is the accuracy of numerical computation due to mesh discretization. The accuracy of the FE solution affects directly on the exactness of the prediction of the crack propagation trajectory. Adaptive mesh refinement is an appropriate technique to control the discretization error especially in the near crack tip region. However, the optimal mesh configuration changes continually throughout the crack growth and several stages of mesh refinement may be required. Since the exact solution is usually not available in most of crack problems, it is approximated by a recovered solution to estimate the error. Zienkiewicz and Zhu (1987) introduced recovery-based error estimation to obtain more accurate representation of the variables through a recovery procedure. One of the most accurate recovery based techniques was superconvergent recovery (SPR) technique introduced by Zienkiewicz and Zhu (1992). They assumed a polynomial expansion for stress field over a patch of elements sharing each node and then interpolated those nodal values using standard shape functions to obtain the recovered stress values. Moslemi and Khoei (2009) improved this technique to Weighted SPR considering different weighting factors for superconvergent points of the patch. This technique estimated the error more efficient and realistic particularly in the boundaries of problem and elements located near the crack front. Özakça (2003) compared different error estimators in adaptive finite element analysis of linearly elastic structures based on flux projection or best guess stress values and residual methods. Ullah *et al*. (2013) developed an automatic adaptive coupling procedure combining finite element method and element free Galerkin method (EFGM). They converted the elements which violate a predefined error measure to an EFG zone avoiding computationally expensive FE remeshing.

Ródenas *et al*. (2013) enhanced the error estimation in energy norm using a moving least squares recovery based procedure. This technique was more flexible than SPR techniques as it directly provided continuous interpolated fields without relying on any FE mesh. A goal oriented error estimation in the extended finite element method was proposed by González-Estrada *et al*. (2015) which considered the stress intensity factor as the quantity of interest. Chen *et al*. (2016) presented a Three-dimensional superconvergent gradient recovery on tetrahedral meshes based on centroidal Voronoi Delaunay tessellations (CVDT). They established a modified superconvergence patch recovery method to overcome the influence of slivers on CVDT meshes. An adaptive higher-order method based on a generalization of polynomial/rational splines over hierarchical T-meshes (PHT/RHT-splines) was introduced by Anitescu *et al*. (2018). They used hierarchical bases and adaptivity and added more degrees of freedom only where they are necessary to improve the approximation. A Statistical Approach for Error Estimation in Adaptive Finite Element Method was proposed by Moslemi and Tavakkoli (2018). They compared the statistical distribution of the stress values at Gauss points around a node with the uniform distribution function to estimate the error. Gibert *et al*. (2019) combined the extended finite element method and automatic adaptive mesh refinement taking advantage of both methods. The enrichment of the model was included in the kinematic continuity relations and the field transfer process. A near-tip grid refinement is introduced by Cho (2019) in the crack analysis by natural element method. This refinement technique is completed in two steps in which grid points are added and Delaunay triangles sharing the crack tip node are divided. Ziaei and Moslemi (2020) presented a new probabilistic error estimator considering uncertainties in geometric sizes, material properties and loading conditions to reduce the mesh dependency of the responses dispersion.

In the present study, the adaptive mesh refinement is employed in the polygonal-FEM for modeling of crack propagation problems. To predict the crack growth, linear elastic fracture mechanics (LEFM) is assumed. A-posteriori error estimator is used based on the Zienkiewicz–Zhu method in conjunction with a weighted SPR technique to obtain the mesh density. The mesh refinement is accomplished generally on the polygonal elements with an arbitrary mesh density. To prevent poor polygonal element shapes, local modifications are applied on the mesh in the steps that the estimated error are kept within the prescribed error. The crack growth process is accomplished independent from the mesh refinement procedure and the mesh is refined in some steps of crack growth which the estimated error violates a predefined error measure. This study is the first to specifically investigate the mesh adaptivity with the estimated error in polygonal elements and distribute the error uniformly across the domain with arbitrary mesh density. In the previous researches on polygonal finite element method, the mesh was modified locally and a very fine mesh was employed near the crack tip zone to reduce the discretization error. The remainder of this paper is organized as follows. Section 2, reviews interpolants functions of polygonal elements and numerical integration on polygons. Next, in Section 3, an adaptive mesh refinement strategy is introduced for polygonal elements in crack growth problems. In order to illustrate the capability of proposed approach in crack propagation problems, several numerical simulation results are presented in Section 4. Finally, some concluding remarks are given in Section 5.

2. Polygonal finite element method

2.1 Shape functions for polygonal domains

Researchers have recently become interested in using *n*-sided polygonal elements in finite element modeling of mechanical and structural components. There are several approaches to represent the shape functions over polygonal elements satisfying essential conditions. These essential conditions include local support, inter-element compatibility, Lagrange property and completeness (Khoei *et al*. 2015). In the most commonly used approaches, the weight functions are employed to construct the shape functions as

$$N_j(x) = \frac{w_j(x)}{\sum_{i=1}^{n} w_i(x)} \tag{1}$$

In a trigonometric form of the approach presented by Meyer *et al*. (2002), the weighting functions for node *j* defined as

$$\widehat{w}_j = \frac{S(p_i, p_j, p_k)}{S(p, p_i, p_j)S(p, p_j, p_k)} = \frac{\cot(\beta_j) + \cot(\alpha_j)}{\|x_j - x\|^2} \tag{2}$$

where p_i, p_k are adjacent nodes to the node *j*, p is the interpolation point and *S* denotes the area of the triangle whose vertices are specified in the parentheses. The norm $\|x_j - x\|^2$ is the distance between interpolation point and node *j* and the angles β_j and α_j are indicated in Fig. 1. This definition would result non-negative shape functions for convex polygons.

To compute the stiffness matrix of each element, the derivatives of these shape functions should be integrated over the element. To approximate the integrals by a Gaussian form of numerical quadrature in polygonal domains, a virtual node is assumed within the element and it is connected to real nodes of the element. Thus, the polygonal element is partitioned into triangular elements and Gauss quadrature points of these triangular elements are used for numerical integration as shown in Fig. 2. The local coordinates of Gauss quadrature points in sub-triangles have been adjusted according to the barycentric coordinates of the polygonal element.

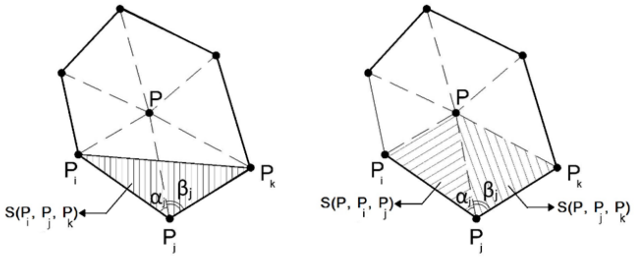

Fig. 1 Parameters of the polygonal shape functions

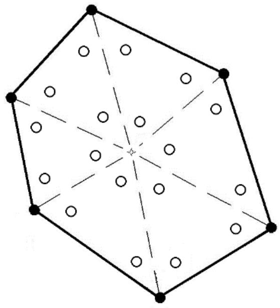

Fig. 2 Gauss qudrature points of sub-triangles in numerical integration

2.2 Polygonal mesh generation

In adaptive remeshing procedure, many constraints are exerted on elements size over the domain. These paradoxical constraints in triangular and quadrilateral meshes may produce ill-shaped elements and result high values of error. Polygonal discretization offers greater flexibility in mesh generation particularly in complicated geometries. The most common polygonal discretization algorithms are based on the Voronoi diagrams and their reflections. In this study, PolyMesher (Talischi *et al*. 2012) written for the polygonal mesh generation is employed and modified for interfering element in crack propagation models. This algorithm is mainly based on the implicit description of the domain and the centroidal Voronoi tesselleation (CVT). Defining signed distance function, any arbitrary domain can be specified by separating internal and external points of the domain. If the domain is denoted by Ω, the signed distance function which represents the nearest distance from boundary is defined by:

$$d(x) = s(x) \min_{y \in \partial\Omega} \|x - y\| \tag{3}$$

where $\partial\Omega$ is the boundary of Ω, $\|x - y\|$ denotes the distance between *x* and point *y* on the boundary of the domain and the sign function is given by:

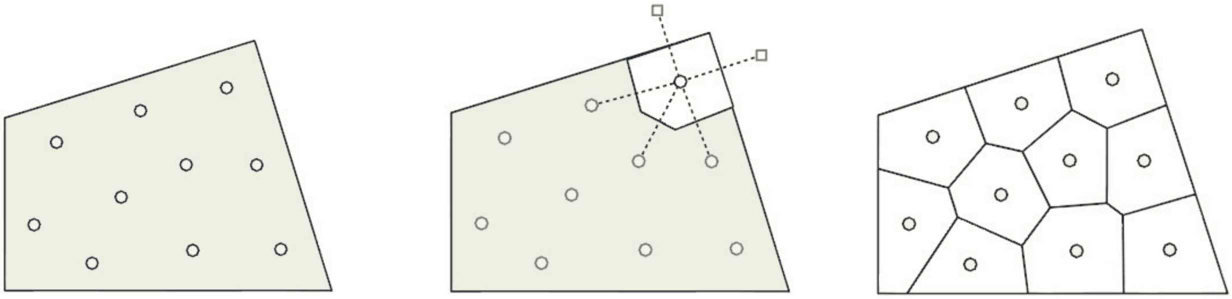

Fig. 3 Polygonal mesh generation procedure (Talischi *et al*. 2010)

$$s(x) = \begin{cases} -1, & x \in \Omega \\ +1, & x \notin \Omega \end{cases} \tag{4}$$

Thus, the points are categorized to internal, boundary and external points of the domain as:

$$\Omega = \{x \in R^2 : d(x) < 0\}$$
$$\partial\Omega = \{x \in R^2 : d(x) = 0\} \tag{5}$$
$$\overline{\Omega} = \{x \in R^2 : d(x) > 0\}$$

The seeds which represent the mesh density are placed in the domain. Then these seeds are reflected with respect to the boundary using signed distance function. The domain is partition to the cells using Voronoi diagram where each point of the cell has the smallest distance to the corresponding seed of the cell. A schematic process of mesh generation is illustrated in Fig. 3.

A random selection of the seeds may lead to a polygonal mesh not suitable for use in finite element analysis. Thus, an iterative algorithm is proposed to modify the generating seeds location. Lloyd algorithm replaces the given generators by the centroids of the corresponding Voronoi regions iteratively. These iterations decrease an energy functional and the process continues until the seeds are mapped to themselves.

3. Adaptive polygonal mesh refinement in crack growth problems

3.1 Adaptive mesh refinement

Since the critical points of the problem change continuously through the crack growth steps, the polygonal mesh should be refined in some steps of crack growth to control the discretization error. However, to reduce the computational cost, the remeshing process is accomplished only in steps which the estimated error exceeds the aim error. In crack growth problems, the mesh refinement is needed when the crack tip gets away from the previous refined region. Since the exact solution of the problem is unknown in most problems, the error is estimated using a recovered solution.

$$e_\sigma \approx \sigma^* - \hat{\sigma} \tag{6}$$

where $\hat{\sigma}$ represents the stress value obtained from FE solution and σ^* is the recovered stress. The recovered stress is estimated by interpolating a polynomial function over a patch of elements surrounding each nodal point. Thus, a component of recovered stress σ_i^* is given by

$$\sigma^*{}_i = \mathbf{Pa} = \langle 1\; x\; y \ldots\; y^n \rangle \langle a_0\; a_1\; a_2 \ldots\; a_n \rangle \tag{7}$$

The unknown vector **a** is obtained by a least square fit to the finite element solutions over the patch. According to the technique proposed by Moslemi and Khoei (2009), different weighting factors are assumed for sampling points in the error function to make a more realistic recovered stress. This technique improves the recovering procedure particularly in regions with high gradient of stress such as the crack tip zone. Thus, the error function takes the following form:

$$\begin{aligned} \mathrm{F}(\mathbf{a}) &= \sum_{k=1}^{n} \left(w_k [\sigma^*{}_i(x_k, y_k) - \sigma^\wedge{}_i(x_k, y_k)] \right)^2 \\ &= \sum_{k=1}^{n} \left(w_k [\mathbf{P}(x_k, y_k)\boldsymbol{a} - \sigma^\wedge{}_i(x_k, y_k)] \right)^2 \end{aligned} \tag{8}$$

The weighting factors are considered in terms of the distance of the sampling points from the recovering node. Thus, the nearest sampling points have more effect in the recovery process. If r_k denotes the distance of k-th sampling point form the recovering node, the corresponding weighting factor is taken as $w_k=1/r_k$. After determination of the recovered polynomial, the nodal recovered stress is computed by the evaluation of the polynomial at the nodal coordinates. The recovery process is accomplished for all of the nodes of the mesh. Since the finite element solution has been computed on Gauss quadrature points, the recovered solution is transferred from nodal points to Gauss points using Wachspress shape functions as it was described in Section 2.

$$\sigma^* = N.\bar{\sigma}^* \tag{9}$$

where $\bar{\sigma}^*$ represents the nodal recovered stress. The recovery stress procedure in polygonal elements is illustrated in Fig. 4.

The error is estimated over the domain as the difference of the recovered stress and finite element solution according to Eq. (6). The region with high stress gradient show the larger values of error and the uniform stress regions have smaller error. A strategy to have an optimal mesh is to distribute the error uniformly over the elements. Thus, to attain the uniform error, the mesh is refined in regions with

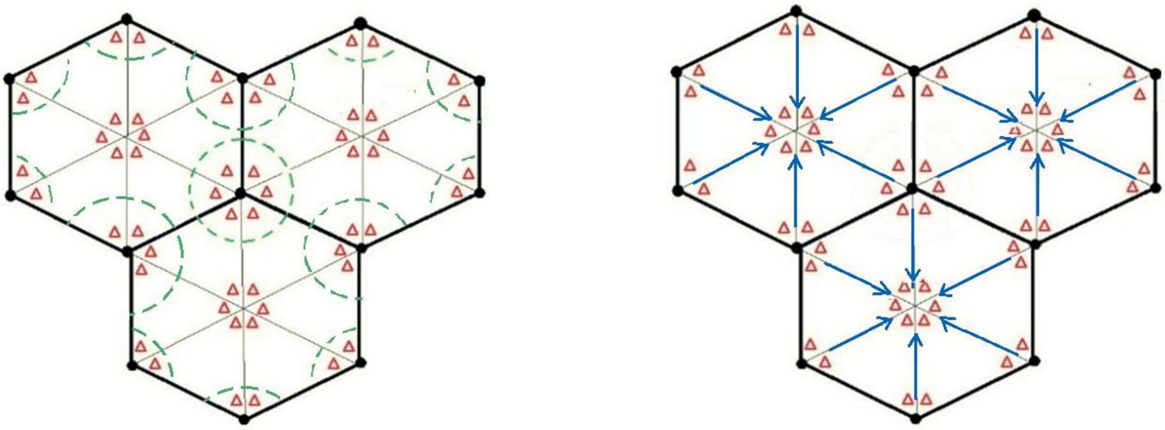

Fig. 4 The process of recovering of the stresses on polygonal elements; ● nodal points, Δ Gauss points; dashed circles represesnt the patch of the recovering node and blue arrows indicate the process of stress transfer from nodal points to Gauss points

high error and the elements are coarsened in regions with low error. To make the error dimensionless, it is normalized with respect to the overall average stress. This average stress is achieved by weighted averaging of stress over all of the elements.

$$\eta = \frac{\|e_\sigma\|}{\|\hat{\sigma}\|} \tag{10}$$

Now if η_{aim} represents the aim error, the new size for mesh refinement would be determined by:

$$(h_i)_{new} = (\frac{\eta_{aim}}{\eta})(h_i)_{old} \tag{11}$$

where $(h_i)_{old}$ and $(h_i)_{new}$ denote i-th element size in previous mesh and refined mesh, respectively. Repeating this procedure for all of the elements would produce the refinement mesh density. Since the polygonal mesh is generated by a set of Voronoi seeds, first a background triangular mesh is generated according to the refinement mesh density and then, the nodes of this triangular mesh is utilized as the seeds for PolyMesher.

The estimated pointwise error is always larger than aim error in singular points such as the crack tip. Thus, this pointwise error is not a proper criterion for mesh refinement and a global error estimation over the domain is needed. Comparing the global estimated error with the aim error indicates that the mesh refinement is not required in all steps of the crack growth and a local modified mesh could be used in several steps of the crack growth. To evaluate the overall error, Gauss point errors are integrated over all of the elements.

$$\|e_\sigma\| = \left(\int_\Omega (\sigma^* - \hat{\sigma})^T(\sigma^* - \hat{\sigma})\, d\Omega\right)^{1/2} \tag{12}$$

A multilevel mesh refinement is required, when the error is not attained the aim error in first level. After attaining the aim error, the finite element solutions are reliable and the crack growth is accomplished according to these results. In this study, maximum circumferential tensile stress criterion is used to find the direction of the crack growth (Erdogan and Sih 1963).

3.2 Local remeshing procedure

Although the aim error would be attained in some steps of the crack growth and no mesh refinement is required, however, local modifications are applied on the mesh to prevent poor polygonal element shapes. Since a few elements are intersected by the crack growth line, negligible computational cost is imposed in this procedure. When the crack intersects an element side, the element is splitted in two distinct elements. However, if the intersection point is very close to the node, a poor element with very small side would be created. If d denotes the distance of the intersection point and the node and L represent the element side, the modification is required when $d<\alpha L$. α is a user defined parameter which indicates the sensitivity of the mesh to the small side elements. In this study it is assumed to be 0.2. Small values for α would result ill-shaped elements and deviate the crack path. However, choosing large values for this parameter would require local modification in many elements and impose high computational effort without considerable improvement of the solution. The effect of this parameter on mesh modification is illustrated in Fig. 5 considering three different values for α. For local modification of the mesh, the node is moved to the intersection point to eliminate the small side. The element containing the crack tip is also divided to several elements to prevent from the concave element. The crack tip is connected to peripheral nodes which make element angles smaller than 135°. The local modification procedure for small side elements is illustrated in Fig. 6 as node 7 is transferred to node 19 and then node 16 is connected to nodes 12 and 14.

Another local modification occurs when the crack tip is close to an element side. In this condition a poor element with large angles would be created. Thus, to avoid such elements, the near element side is transmitted to the crack tip location. This modification converts the neighbor element to a critical element and this element should be divided to two distinct elements by connecting the crack tip to peripheral nodes which make element angles smaller than 135°. Fig. 7 shows the local modification process for large angle elements. Overall scheme of the proposed algorithm

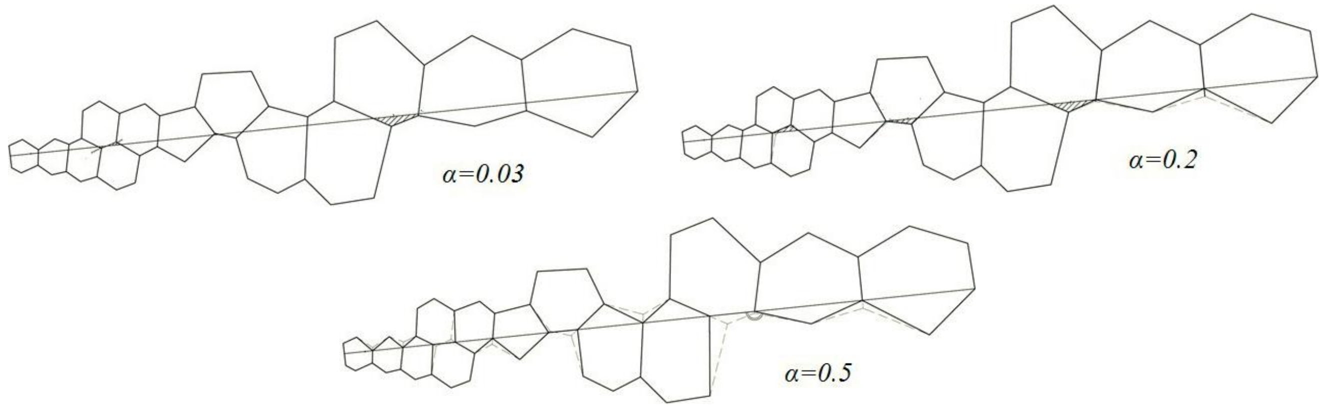

Fig. 5 The effect of parameter α on local mesh modification process

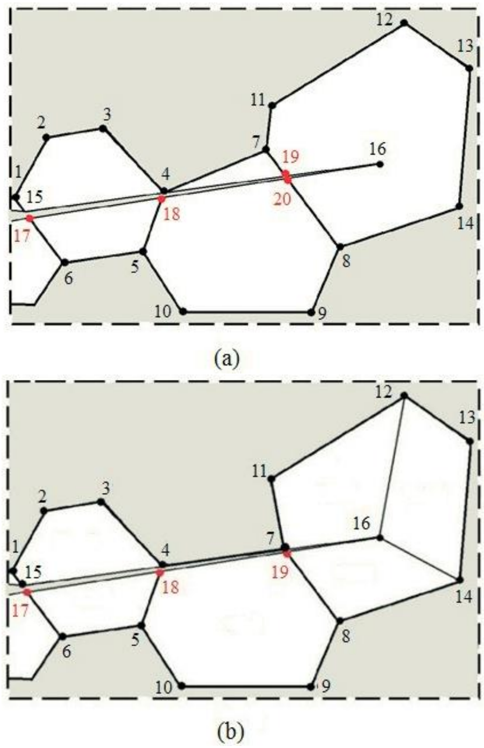

Fig. 6 The local modification procedure for small side elements a) before modifacation b) after modification

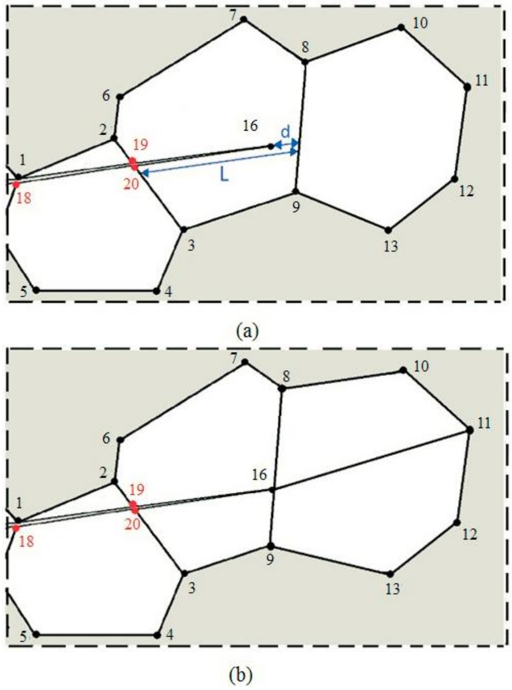

Fig. 7 The local modification procedure for large angle elements a) before modifacation b) after modification

for adaptive polygonal mesh refinement in crack growth problems is summarized in flowchart in Fig. 8.

The proposed algorithm can be generalized to three dimensional problems with a little modification of the procedures. The polygonal mesh generator (Polymesher) should be replaced with a polyhedral mesh generator. In the process of the error estimation, three dimensional polynomials should be employed to recover the stress and finally, a spatial crack growth criteria must be applied. This algorithm is capable of capturing complicated crack patterns in dynamic fractures, including crack branchings and crack coalescence. Employing the dynamic finite element method, a dynamical instability causes oscillations in crack velocity and structure. Applying the mesh adaption, the minor branches may also be captured. The advantage of great flexibility of the polygonal elements would facilitate the crack coalescence.

The computational cost spent in the proposed algorithm consists of three main parts: finite element analysis, error estimation and updated mesh generation. However, the finite element analysis requires greater than 90% of the computational effort and other parts have negligible effect on the computational cost. In the examples of the next section, the error estimation and mesh generation process had taken just a few seconds. Thus, in the proposed algorithm, the time saving achieved through mesh optimization outweighs the cost of adaptive remeshing.

4. Numerical simulation results

To illustrate the capability and performance of proposed adaptive strategy together with the polygonal FEM described in section 3, several numerical examples are presented. The first example is chosen to demonstrate the accuracy of the proposed algorithm for a benchmark

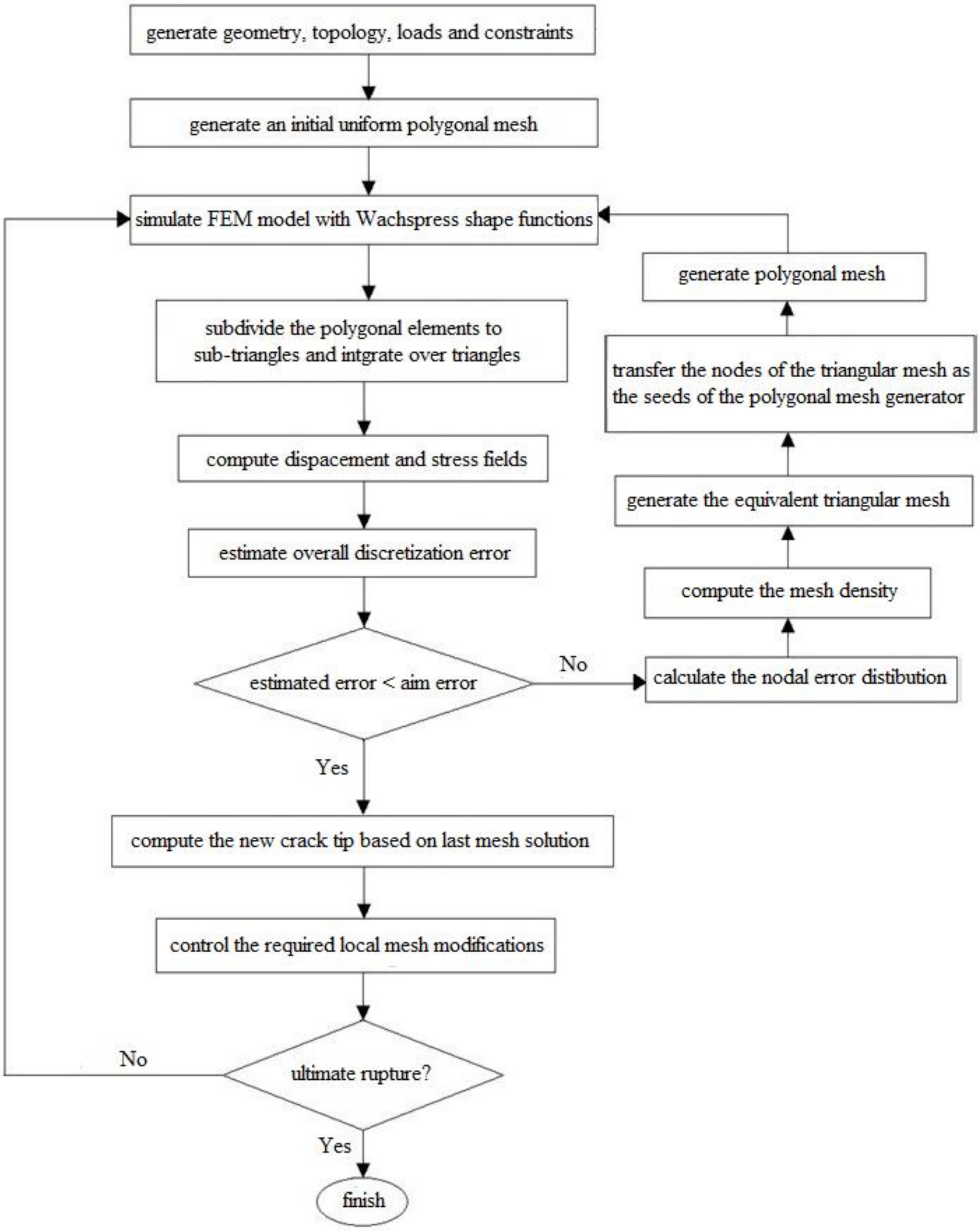

Fig. 8 Flowchart of the adaptive polygonal mesh refinement in crack growth problems

problem in a uniaxial tensile stress. The effect of the implemented adaptive strategy is shown on the predicted crack path. The complex geometries are chosen for the next two examples to challenge the capability of the algorithm in such problems. To determine the crack growth direction, the maximum circumferential stress criterion is employed. The crack grows with a pre-defined constant length at each step of crack propagation. This length determines the number of crack growth steps and required computational effort. To optimize the computational cost, larger crack growth steps are taken in direct crack paths and this length is decreased when the crack kinks suddenly. All examples are modeled by a plane strain condition and the first order polygonal elements are employed for the finite element meshes. The

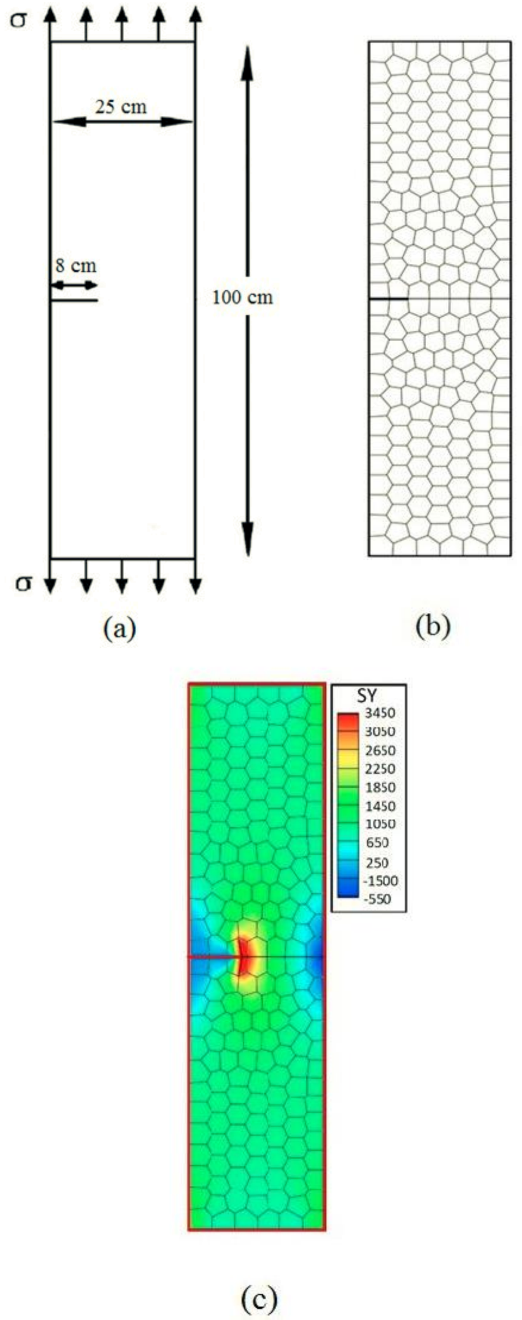

Fig. 9 The rectangular plate with an edge crack in tension; a) geometry and boundary conditions b) initial FE mesh c) the contour of stress σ_y

adaptive strategy has been initialized with a coarse uniform polygonal FE mesh in all of the examples. The error estimation procedure was used based on the Zienkiewicz-Zhu error estimator. The different values for aim error are considered depending on the nature of the problem. The value of the aim error is determined by the user and depends on the acceptable error. It is usually taken 10% in the literature. Small values of the aim error would increase remeshing steps and computational effort. However large values of the aim error may result inaccurate crack growth modeling. In the following examples the aim error is adjusted in a way that there would be at least two adaptive remeshing stages in all of the examples. The variation of estimated error with crack length is illustrated during adaptive mesh refinement to investigate the efficiency of error estimation and mesh refinement procedures. The initial and refined meshes are shown during the adaptive remeshing procedure. The entire process of adaptive mesh refinement has been automatically performed without user intervention. To demonstrate the accuracy of the proposed algorithm, the results are compared with those reported in literature.

4.1 A rectangular plate with an edge crack in tension

The first example refers to tensile loading of a rectangular plate with an edge crack as shown in Fig. 9(a). This example is chosen to illustrate the performance of adaptive polygonal mesh refinement strategy for a benchmark problem. The top and bottom edges of plate are subjected to uniform vertical traction $\sigma = 1000\ kgf/cm^2$. The elasticity modulus of the plate is $E = 2\times10^6\ kgf/cm^2$ and the Poisson ratio is $\nu = 0.3$. The plate is initially modeled and meshed with 200 uniform five-sided and six-sided elements as shown in Fig. 9(b).

The FE analysis of the initial mesh illustrates the stress concentration at the crack tip as shown in Fig. 9(c). To demonstrate the performance of the proposed algorithm, the crack is propagated using adaptive polygonal FEM and classic FEM. In the classic approach the analysis is accomplished on the base of the initial mesh. However, in the adaptive approach the model is remeshed as the estimated error exceeded the aim error. In this example the aim error is taken 6% and the crack growth length is 2 cm. In both approaches the error estimated in different crack growth steps. The trend of estimated error in these approaches are summarized in Table 1. It can be seen that in two steps of the crack growth (steps 2 and 6) the estimated error exceeds the aim error and adaptive remeshing is required. In other five steps the aim error is satisfied and the crack is propagated according to the previous mesh. However, a minor tolerances in number of elements can be seen in these five steps, due to the local modification described in Section 3.

The process of adaptive mesh refinement in steps 2 and 6 are illustrated in Fig. 10. The contour of estimated error indicates that the crack tip region contains highest values of error and a uniform mesh cannot satisfy accuracy conditions. Thus, a refined mesh near the crack tip zone is generated (Fig. 10(c)) and the mesh is coarsened in low error regions. In next four steps, the current mesh (Fig. 10(d)) have satisfied accuracy conditions. However, in step 6 as the crack tip takes some distance from refined zone, another adaptive mesh refinement is required to reduce the estimated error to aim error. Thus the refined zone moves to the right part of the plate (Fig. 10(f)) and the previous refined zone have coarsened. Since the large parts of the domain is coarsened in this step, the number of element and nodes have been reduced after mesh refinement from 1145 to 997 (Table 1). This implies that the proposed mesh refinement procedure may decrease the computational effort in some problems.

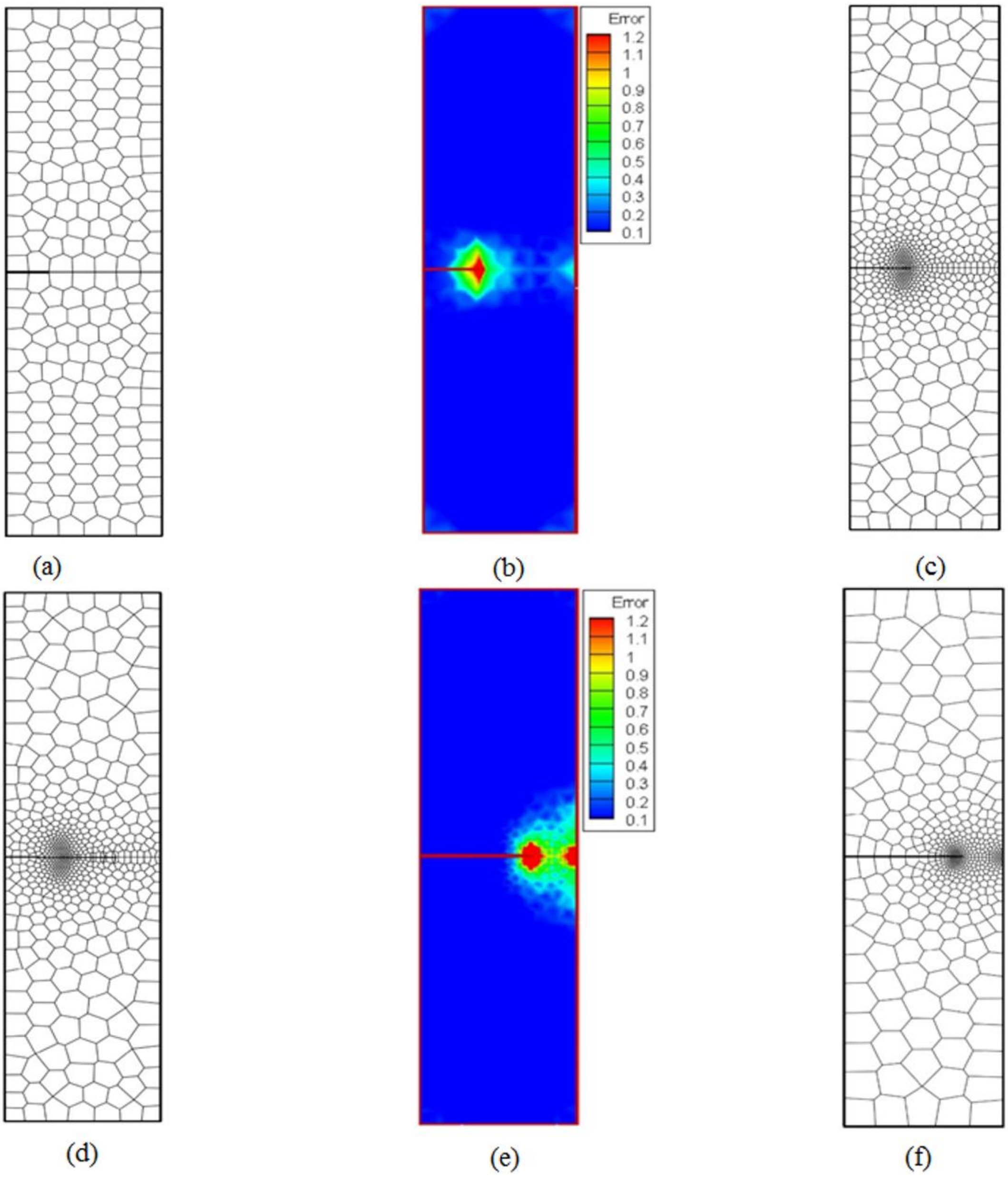

Fig. 10 The rectangular plate with an edge crack in tension; a,d) The FE mesh before refinement, b,e) the estimatederror contour, c,f) the refined FE mesh in steps 2 and 6 of crack growth

In Fig. 11, the variation of the estimated error during the crack growth is shown for the uniform and adapted meshes. In the classic method without mesh refinement, the estimated error is increased in consecutive steps which makes the results unreliable. In each step the error takes the crack into mixed mode and intensifies the error in next steps. However, in adaptive polygonal FEM the error is controlled whenever it exceeds the target error. The maximum circumferential stress criterion is employed.in both methods for the kinking angle of the crack. The adaptive method propagates the crack in a straight line as it was expected. However, in the classic method without mesh refinement, the large value of stress error result in a deviation of crack path. The crack trajectory obtained using the adaptive FE technique is compared with the classic method in Fig. 12.

4.2 Mixed mode crack propagation in the bending beam with three holes

The second example is of a rectangular Plexiglas bending beam weakened by three holes as shown in Fig. 13(a). The presence of holes in the plate disturbs the stress field around the holes which result to curvilinear crack path. This path is highly dependent on the initial crack size and its position. This example have been investigated experimentally and numerically by different researchers (Bittencourt *et al*. 1996, Khoei *et al*. 2015) to show the performance of their proposed computational algorithm. In this example the crack size and eccentricity is chosen $a=1$ *in* and $b=6$ *in*. The experimental results indicates that the crack intersects the middle hole in this case. The material properties of Plexiglas is chosen as follows; $E=348076$ *psi* and $v= 0.3$. The FE modeling have been initiated with 232

Table 1 The rectangular plate with an edge crack in tension; Summary of estimated errors for adaptive polygonal FEM and classic FEM

	Adaptive polygonal FEM			Classic FEM		
Crack growth step	Number of elements	Number of nodes	Estimated error (%)	Number of elements	Number of nodes	Estimated error (%)
1	200	396	4.98	200	396	4.98
2	202	398	6.20	202	398	6.20
2 (remeshed)	594	1126	2.35	-	-	-
3	596	1132	3.33	204	401	9.89
4	598	1137	4.44	204	402	11.85
5	600	1141	5.59	206	404	13.39
6	602	1145	6.67	206	405	16.14
6 (remeshed)	524	997	1.33	-	-	-
7	524	1002	1.51	208	407	19.86

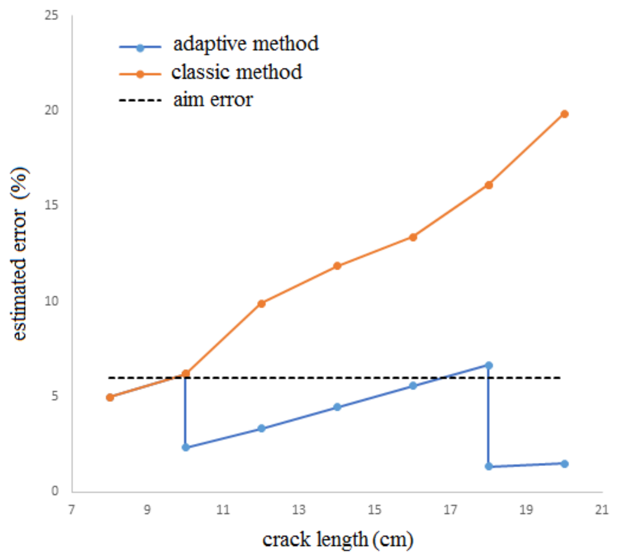

Fig. 11 The rectangular plate with an edge crack in tension; The variation of overall percentage of estimated error with crack length

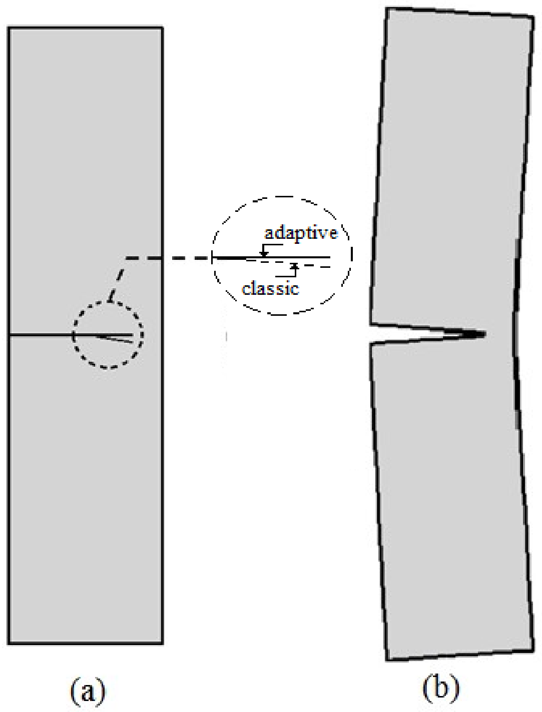

Fig. 12 The rectangular plate with an edge crack in tension; a) a comparison of the crack path between the uniform and adapted meshes, b) the deformed shape of the crack growth

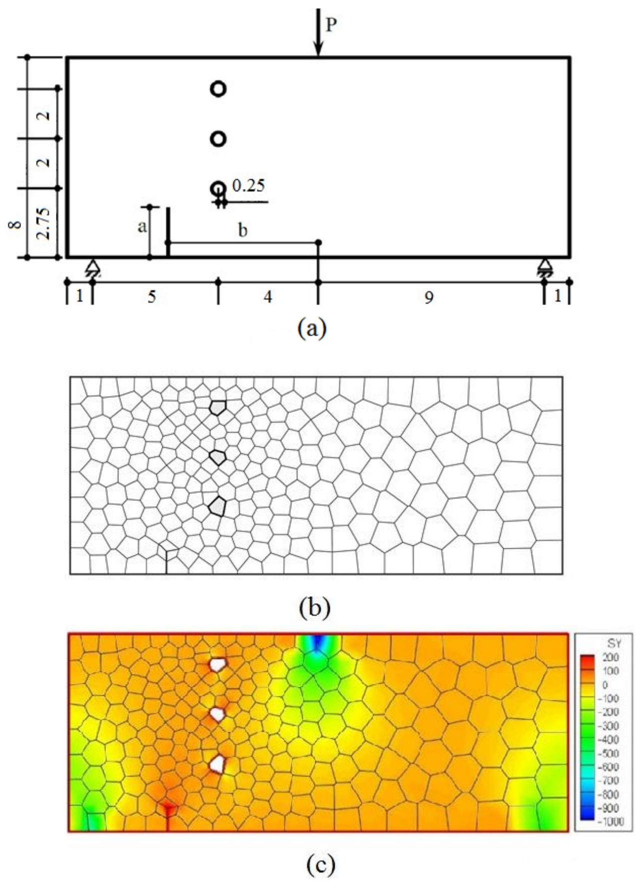

Fig. 13 Bending beam weakened by three holes; a) geometry and boundary conditions (all dimensions in inch), b) initial FE mesh mesh, c) the contour of stress σ_y

polygonal elements as shown in Fig. 13(b). The initial analysis indicates that this example have several critical points which show stress concentration in regions such as crack tip, point load, constraints and near hole zone as shown in Fig. 13(c).

The aim error is chosen 7% to necessitate three adaptive steps. The trend of the estimated error is summarized in Table 2. Since the initial mesh is coarse and the holes are modeled roughly (Fig. 13(b)), the adaptive refinement is required from the very first step of analysis which shows largest value of error (12%). Two additional adaptive remeshing have accomplished in steps 3 and 5 where the aim error is not achieved. Different crack growth lengths have been considered in various steps depending on the kinking of the crack. The procedure of adaptive polygonal remeshing is illustrated in Fig. 14. The initial meshes (Figs. 14(a)-(c)) are improved (Figs. 14(g)-(i)) according to error

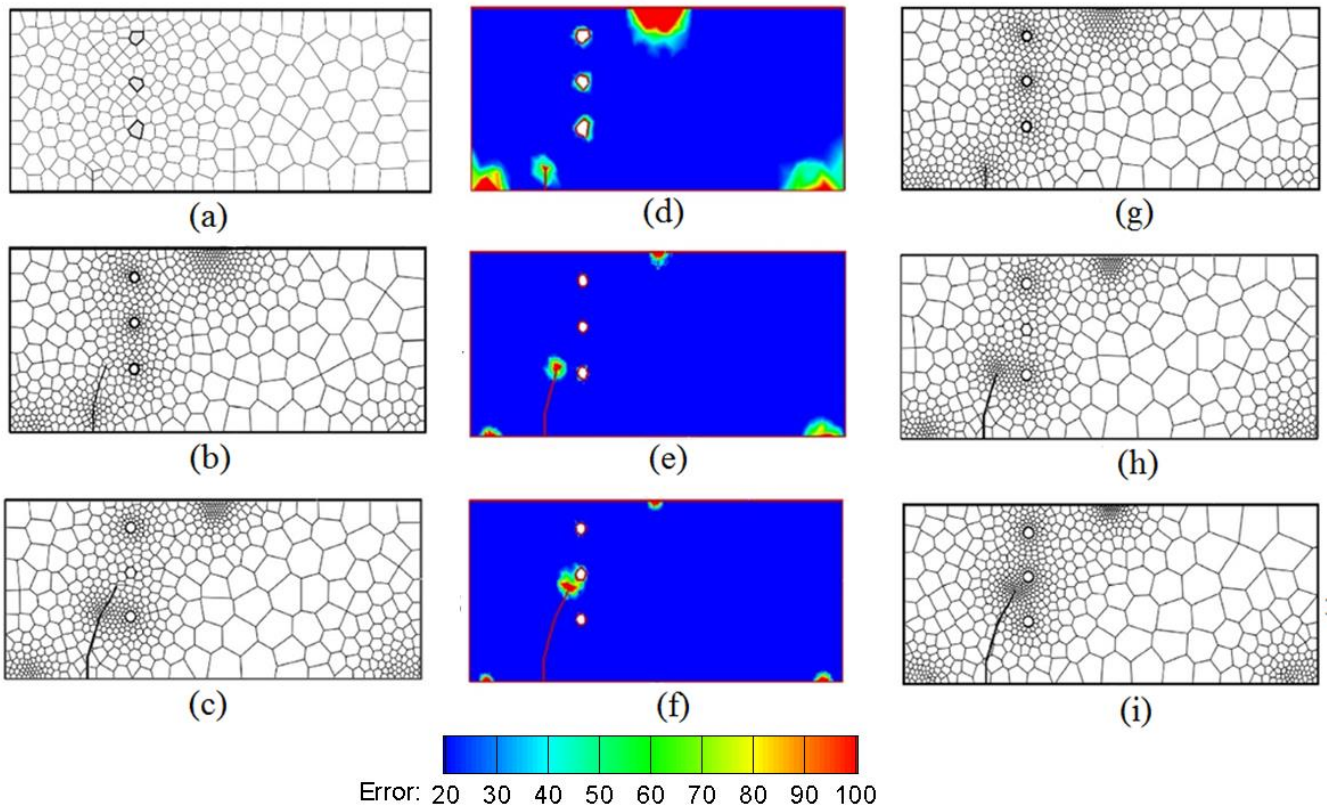

Fig. 14 Bending beam weakened by three holes; a-c)The FE mesh before refinement, d-f)the estimated error contour, g-i)the refined FE mesh at steps 1,3 and 5 of crack propagation respectively

contours (Figs. 14(d)-(f)). In early stages, the side holes are more refined due to the crack tip and point load. However, in last stages the as the crack grows, the middle hole becomes more critical and requires higher dense mesh.

An important aspect of the adaptive FEM is to create an optimal mesh with minimum degrees of freedom while producing an error value that is lower than the aim error. In traditional adaptive mesh refinement with triangular or quadrilateral elements, the remeshing procedure usually increase number of DOFs drastically. However great flexibility of mesh generation in polygonal elements controls the number of DOFs and makes the polygonal adaptive FEM more efficient. It is obvious from Table 2 that the number of nodes is not increased considerably. The convergence of the estimated error is depicted in Fig. 15 for successive FE meshes. The drops on the graph indicates the effect of adaptive mesh refinement on the discretization error.

The eccentricity of the crack and the presence of the holes diverts the crack toward the holes and results the mixed mode crack propagation. The crack path is predicted using the maximum circumferential stress criteria and is compared to those of experimental and numerical results reported by Bittencourt *et al*. (1996) (Fig. 16(a)). A good agreement can be seen between the numerical prediction and those of experiments. The crack growth length is reduced to *0.3 in* where the crack curves sharply in final steps of crack propagation. Fig. 16(b) indicates that the crack ultimately intersects the middle hole as it was observed in the experimental tests (Bittencourt *et al*. 1996).

Table 2 Bending beam weakened by three holes; Summary of estimated errors for adaptive polygonal FEM during crack growth

Crack growth step	Crack growth length (in)	Number of elements	Number of nodes	Crack length (in)	Estimated error (%)
1	1.5	232	465	1	12.12
1 (remeshed)	1.5	605	1204	1	3.68
2	0.5	611	1215	2.5	6.88
3	0.5	611	1219	3	7.83
3 (remeshed)	0.5	616	1247	3	5.20
4	1	617	1250	3.5	6.30
5	0.25	622	1256	4.5	10.24
5 (remeshed)	0.25	672	1343	4.5	5.39
6	0.25	676	1349	4.8	5.95
7	0.25	678	1353	5.1	6.20

Khoei *et al*. (2015) predicted the same path with polygonal elements which was highly refined near the crack tip and holes without adaptive remeshing.

4.3 A rectangular plate with cracks emanating from holes

The last example represents a 10×20 mm rectangular steel plate with two holes as shown in Fig. 17(a). Two cracks oriented with the angle of 45º have emanated from

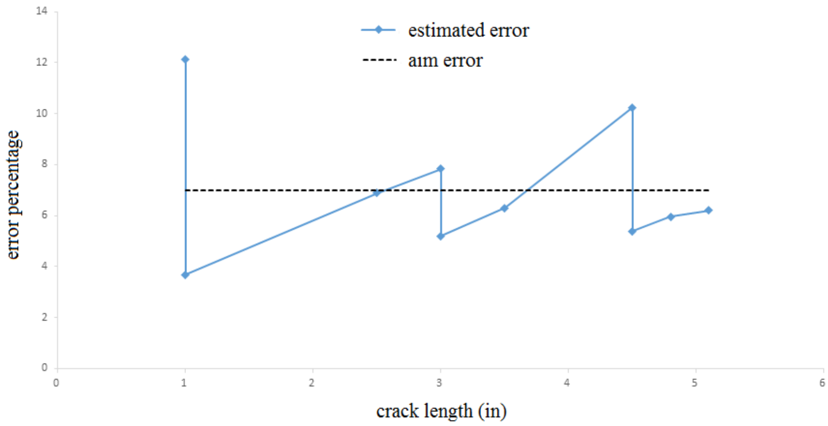

Fig. 15 Bending beam weakened by three holes; The variation of overall percentage of estimated error with crack length

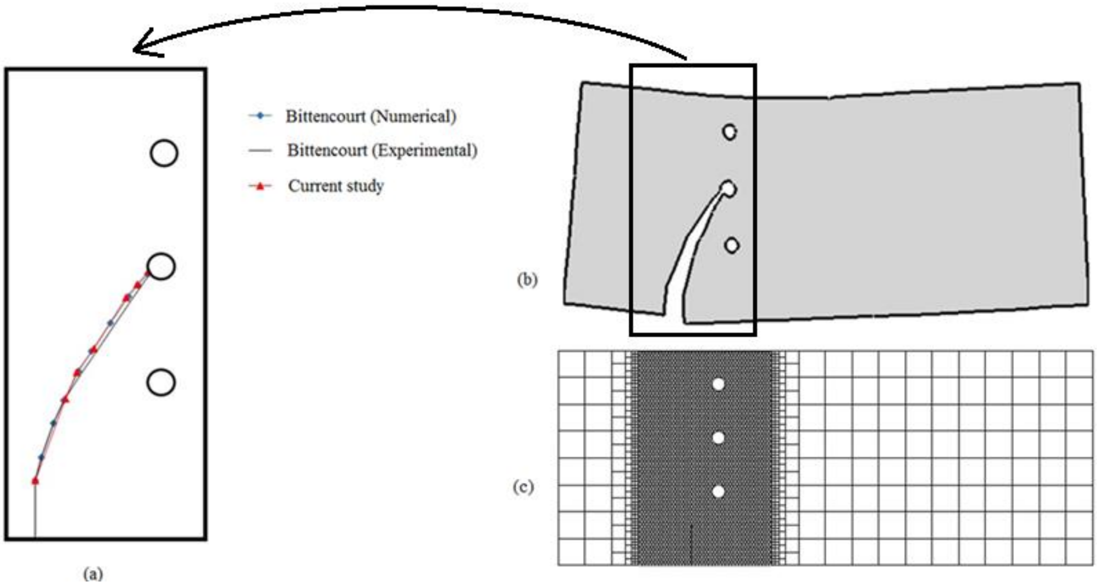

Fig. 16 Bending beam weakened by three holes; a)a comparison of the crack path between the proposed algorithm and experimental results(Bittencourt *et al*.1996) b) the deformed shape of the crack growth, c) the polygonal mesh employed by Khoei *et al*. (2015)

the holes. The problem has been analyzed with displacement control by pulling the top edge of the plate in an incremental manner. The material properties used in this example are the same as the first example. This example is chosen to demonstrate the ability of the proposed algorithm in the problems with multiple cracks. This problem was investigated by Belytschko *et al*. (1995) using element-free Galerkin method. The domain is initially discretized using 204 polygonal elements as shown in Fig. 17(b). The stress concentration can be observed in the crack tips and around the holes. The contour of stress σ_x in step 6 of crack growth is plotted in Fig. 17(c) which indicates the critical regions of the problem. The distributed loading and constraint prevent the stress concentration in top and bottom edges.

The presence of two different cracks will intensify the discretization error and the aim error is taken 10% in this example. The procedure of adaptive remeshing, number of nodes and elements in each step and corresponding estimated errors are summarized in Table 3. The advantage of the polygonal elements is used in half steps of the crack growth and the crack is propagated with previous meshes. However, in steps 1, 4, 6 the aim error has been exceeded and the adaptive remeshing is accomplished. The process of adaptive mesh refinement is illustrated in Fig. 18. Each refined mesh in each step is employed as the initial mesh of next step as shown in Fig. 18. The contour of estimated error (Figs. 18(b),(e),(h)) indicates the regions which require dense mesh. However, the error of these regions are gradually decreased and new critical regions are produced in consecutive steps.

The variation of estimated error with crack length is plotted in Fig. 19. It can be seen the estimated error has approximately linear relation with crack growth. As the crack grows, the crack tip takes some distance from refined zone and the discretization error increases. This relation can be used to roughly predict the steps which require adaptive mesh refinement. Through this approximation, the aim error and number of adaptive mesh refinement stages can be adjusted to balance the required computational cost and the accuracy of the results. The large increment in the last step

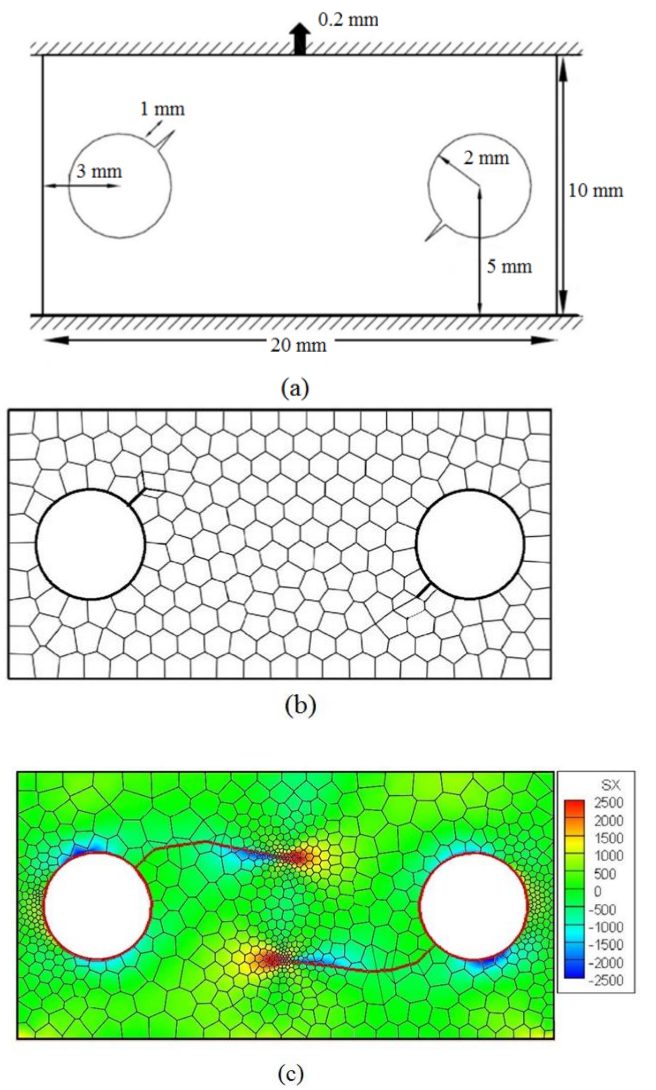

Fig. 17 The rectangular plate with cracks emanating from holes; a) geometry and boundary conditions (all dimensions in mm), b) initial FE mesh mesh, c) the contour of stress σ_x in step6

Table 3 The rectangular plate with cracks emanating from holes; Summary of estimated errors for adaptive polygonal FEM during crack growth

Crack growth step	Crack growth length (mm)	Number of elements	Number of nodes	Crack length (mm)	Estimated error (%)
1	1	204	409	1	10.1
1 (remeshed)	1	499	982	1	5.83
2	0.5	509	996	2	7.74
3	0.5	514	1002	2.5	9.01
4	0.5	518	1007	3	10.6
4 (remeshed)	0.5	738	1462	3	5.97
5	2.5	745	1476	3.5	7.37
6	2.5	758	1496	6	12.94
6 (remeshed)	2.5	805	1585	6	5.26

of crack growth results a long distance between crack tip and refined zone (Fig. 18(g)) and makes maximum estimated error in this step as shown in Fig. 19.

The inclined orientation of the cracks leads to mixed mode crack propagation in initial steps of the crack growth. However, in next steps crack curves to horizontal direction and mode I dominates the crack behavior. Thus, large crack growth length is considered in last modeling steps. In final steps, the cracks attract each other and make an anti-symmetric pattern as shown in Fig. 20. Khoei *et al*. (2008) analyzed this example using an automatic adaptive mesh refinement technique with triangular elements. Fig. 20 indicates the predicted path is identical to the numerical result reported by Khoei *et al*. (2008).

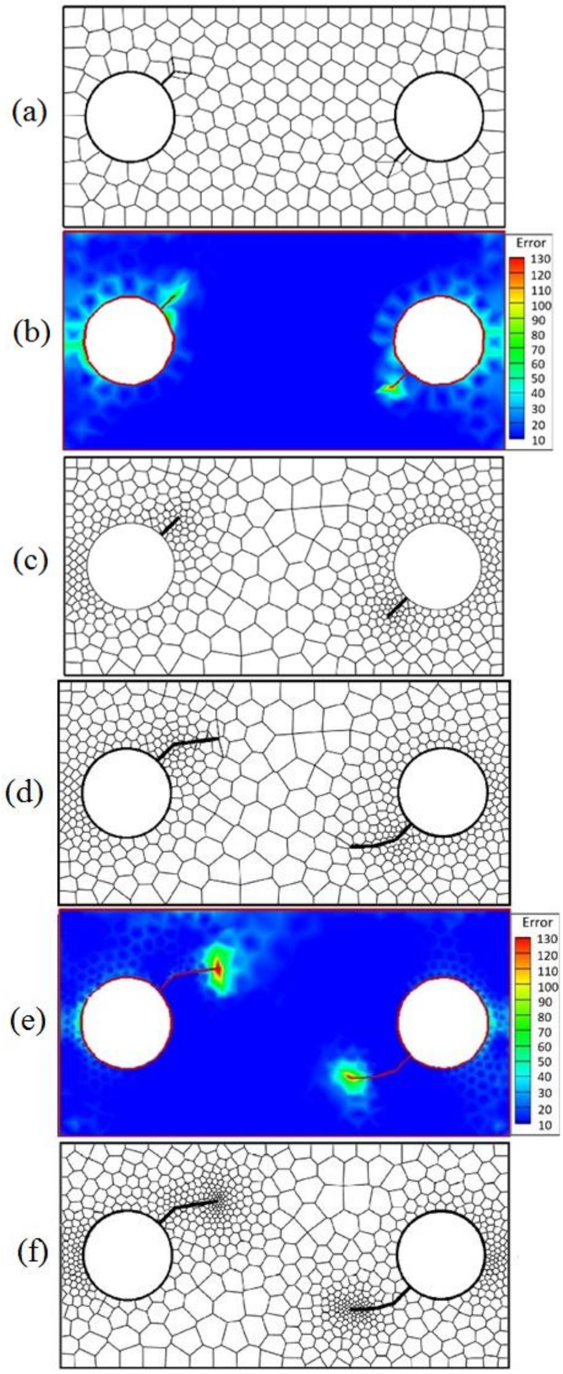

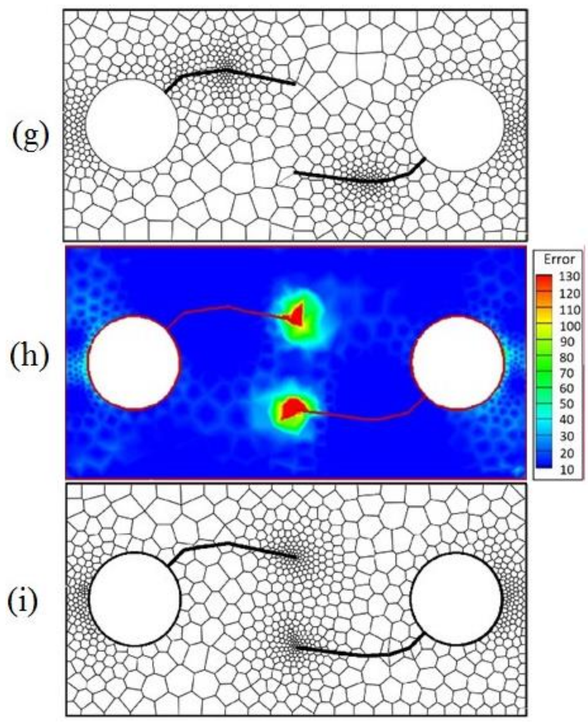

Fig. 18 The rectangular plate with cracks emanating from holes; a,d,g) The FE mesh before refinement, b,e,h) the estimated error contour, c,f,i) the refined FE mesh in steps 1, 4 and 6 of crack growth

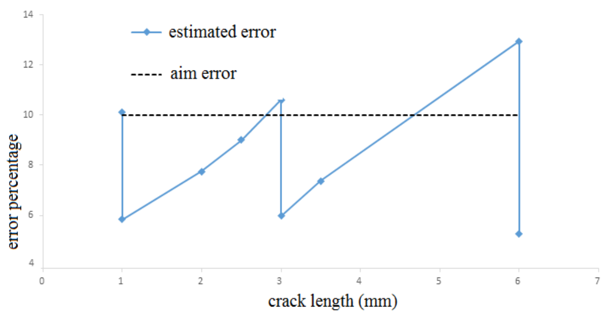

Fig. 19 The rectangular plate with cracks emanating from holes; The variation of overall percentage of estimated error with crack length

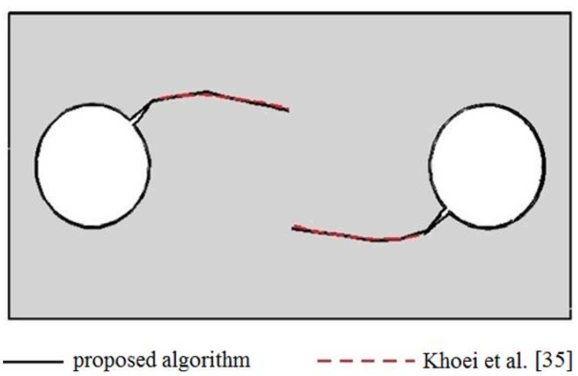

Fig. 20 The rectangular plate with cracks emanating from holes; a comparison of the crack path between the proposed algorithm and those reported by Khoei *et al*. (2008)

5. Conclusion

In the present paper, an automatic adaptive mesh refinement was presented in simulation of crack propagation in the framework of polygonal finite element modeling. The advantage of great flexibility of the polygonal elements was employed to discretize the domain with desired mesh density. In many steps of the crack propagation there was no requirement to overall remeshing and some local modifications was sufficient. This led to huge saving in computational cost of the analysis. In the previous methods, the problem should be analyzed with a very fine mesh in all of the crack growth steps which impose high computational cost to the problem. This is prevented using mesh adaption and reduce the computational cost of the problem. However, in some steps which the crack tip took some distance from the refined zone and the estimated error exceeded the aim error, the proposed adaptive polygonal FEM controlled the error to make FEM solution reliable. Through this procedure the path of the crack propagation was predicted precisely. A linear relation was approximated between the crack growth and estimated error which can be applied for the adjustment of the aim error and computational cost. Very lower number of DOFs was produced during the process of adaptive remeshing in polygonal elements in comparison with triangular and quadrilateral elements as it was reported in the literature (Khoei *et al*. 2008; Moslemi and Khoei 2009) which makes the adaptive mesh refinement more efficient in polygonal elements. Finally, to demonstrate the efficiency and robustness of proposed adaptive algorithm in error reduction, three numerical examples were presented and compared with those available experimental data and analytical solutions reported in literature.

References

Anitescu, C., Hossain, M.N., Rabczuk, T. (2018), "Recovery-based error estimation and adaptivity using high-order splines over hierarchical T-meshes", *Comput. Methods. Appl. Mech. Eng.,* **328**, 638-662. https://doi.org/10.1016/j.cma.2017.08.032.

Beirão Da Veiga, L., Brezzi, F., Cangiani, A., Manzini, G., Marini, L.D., Russo, A. (2013), "Basic principles of virtual element methods", *Math. Models Methods Appl. Sci.*, **23**, 199-214. https://doi.org/ 10.1142/S0218202512500492.

Belytschko, T., Lu, Y.Y., Gu, L. (1995), "Crack propagation by element-free Galerkin methods", *Eng. Fracture Mech.,* **51**, 295–315. https://doi.org/ 10.1016/0013-7944(94)00153-9.

Bittencourt, T.N., Wawrzynek, P.A., Ingraffea, A.R., Sousa, J.L. (1996), "Quasi-automatic simulation of crack propagation for 2D lefm problems", *Eng. Fracture Mech.,* **55**, 321-334. https://doi.org/ 10.1016/0013-7944(95)00247-2.

Chen, J., Chen, Z. (2016), "Three-dimensional superconvergent gradient recovery on tetrahedral meshes", *J. Numerical Methods Eng.,* **108**, 819-838. https://doi.org/ 10.1002/nme.5229.

Cho, J.R., (2019), "Near-tip grid refinement for the effective and reliable natural element crack analysis", *Struct. Eng. Mech.,* **70**(3), 279-287. https://doi.org/ 10.12989/sem.2019.70.3.279.

Dasgupta, G. (2003), "Integration within polygonal finite elements", *J. Aerosp. Eng.,* **16**, 9–18. https://doi.org/10.1061/(ASCE)0893-1321(2003)16:1(9).

Erdogan, F., Sih, G.C. (1963), "On the crack extension in plates under plane loading and transverse shear", *J. Basic Eng.,* **4**, 519–27. https://doi.org/ 10.1115/1.3656897.

Floater, M.S. (2003), "Mean value coordinates", *Comput. Aid. Geometric Design.,* **20**, 19–27. https://doi.org/ 10.1016/S0167-8396(03)00002-5.

Gibert, G., Prabel, B., Gravouil, A. and Jacquemoud, C. (2019), "A 3D automatic mesh refinement X-FEM approach for fatigue crack propagation", *Finite Elements Anal Design.,* **157**, 21-37. https://doi.org/ 10.1016/j.finel.2019.01.008.

González-Estrada, O.A., Ródenas, J.J., Bordas, S.P.A., Nadal, E., Kerfriden, P., Fuenmayor, F. (2015), "Locally equilibrated stress recovery for goal oriented error estimation in the extended finite element method", *Comput. Struct.,* **152**, 1–10. https://doi.org/10.1016/j.compstruc.2015.01.015.

Griffith, A.A. (1921), "The phenomena of rupture and flow in solids", *Philosophical Transactions of the Royal Society*, **221**, 163–198. https://doi.org/ 10.1098/rsta.1921.0006.

Hoshina, T.Y.S., Menezes, I.F.M., Pereira, A. (2018), "A simple adaptive mesh refinement scheme for topology optimization using polygonal meshes", *J. Brazilian Soc. Mech. Sci. Eng.,* **40**, 1-17. https://doi.org/ 10.1007/s40430-018-1267-5.

Hussein, A., Aldakheel, F., Hudobivnik, B., Wriggers, P., Guidault, P.-A., Allix, O. (2019), "A computational framework for brittle crack-propagation based on efficient virtual element method", *Finite Elements Anal. Design*, **159**, 15-32. https://doi.org/10.1016/j.finel.2019.03.001.

Huynh, H.D., Tran, P., Zhuang, X., Nguyen-Xuan, H. (2019), "An extended polygonal finite element method for large deformation fracture analysis", *Eng. Fracture Mech.,* **209**, 344-368. https://doi.org/ 10.1016/j.engfracmech.2019.01.024.

Ingraffea, A.R. (2004), "Computational fracture mechanics", *Encyclopedia of computational mechanics, vol 2*. Wiley, New Jersey. https://doi.org/ 10.1002/0470091355.ecm032.

Khoei, A.R., Azadi, H., Moslemi, H. (2008), "Modeling of crack propagation via an adaptive mesh refinement based on modified superconvergent patch recovery technique", *Eng. Fracture Mech.,* **75**, 2921–2945. https://doi.org/10.1016/j.engfracmech.2008.01.006.

Khoei, A.R., Yasbolaghi, R., Biabanaki, S. (2015), "A polygonal finite element method for modeling crack propagation with minimum remeshing", *Int. J. Fracture,* **194**, 123–48. https://doi.org/ 10.1007/s10704-015-0044-z.

Leon, S.E., Spring, D.W., Paulino, G.H. (2014), "Reduction in mesh bias for dynamic fracture using adaptive splitting of polygonal finite elements", *J. Numerical Methods Eng.***100**, 555–576. https://doi.org/ 10.1002/nme.4744.

Malsch, E.A., Lin, J.J., Dasgupta, G. (2005), "Smooth two dimensional interpolations: a recipe for all polygons", *J. Graphics Tools,* **10**, 27–39. https://doi.org/ 10.1080/2151237X.2005.10129192.

Meyer, M., Lee, H., Barr, A.H., Desbrun, M. (2002), "Generalized barycentric coordinates for irregular n-gons", *J. Graphics Tools***7**, 13–22. https://doi.org/ 10.1080/10867651.2002.10487551.

Moës, N., Dolbow, J., Belytschko, T. (1999), "A finite element method for crack growth without remeshing", *J. Numerical Methods Eng.***46**, 131–150. https://doi.org/ 10.1002/(SICI)1097-0207(19990910)46:1<131::AID-NME726>3.0.CO;2-J.

Moslemi, H., Khoei, A.R. (2009), "3D adaptive finite element modeling of non-planar curved crack growth using the weighted superconvergent patch recovery method", *Eng. Fracture Mech.,* **76**, 1703–1728. https://doi.org/10.1016/j.engfracmech.2009.03.013.

Moslemi, H., Tavakkoli, A. (2018), "A statistical approach for error estimation in adaptive finite element method", *J. Comput. Methods Eng. Sci. Mech.,* **19**, 440-450. https://doi.org/ 10.1080/15502287.2018.1558424.

Ooi, E.T., Shi, M., Song, C., Tin-Loi, F., Yang, Z. (2013), "Dynamic crack propagation simulation with scaled boundary polygon elements and automatic remeshing technique", *Eng. Fracture Mech.,* **106**,1–21. https://doi.org/10.1016/j.engfracmech.2013.02.002.

Özakça, M. (2003), "Comparison of error estimation methods and adaptivity for plane stress/strain problems", *Struct. Eng. Mech.,* **15**, 579-608. https://doi.org/ 10.12989/sem.2003.15.5.579.

Ródenas, J.J., González-Estrada, O.A., Chinesta, F., Fuenmayor, F.J. (2013), "Enhanced error estimator based on a nearly equilibrated moving least squares recovery technique for FEM and XFEM", *Comput. Mech.,* **52**, 321–344. https://doi.org/10.1007/s00466-012-0814-7.

Sibson, R. (1980), "A vector identity for the Dirichlet tessellation", *Mathematical Proceedings of the Cambridge Philosophical Society,* **87**, 151–155. https://doi.org/ 10.1017/S0305004100056589.

Spring, D.W., Leon, S.E., Paulino, G.H. (2014), "Unstructured polygonal meshes with adaptive refinement for the numerical simulation of dynamic cohesive fracture", *Int. J. Fracture,* **189**, 33-57. https://doi.org/ 10.1007/s10704-014-9961-5.

Sukumar, N. (2004), "Construction of polygonal interpolants: a maximum entropy approach", *J. Numerical Methods Eng.,* **61**, 2159–2181. https://doi.org/ 10.1002/nme.1193.

Sukumar, N., Moës, N., Moran, B., Belytschko, T. (2000), "Extended finite element method for three-dimensional crack modelling", *J. Numerical Methods Eng.,* **48**, 1549–1570. https://doi.org/ 10.1002/1097-0207(20000820)48:11<1549::AID-NME955>3.0.CO;2-A.

Talischi, C., Paulino, G.H., Pereira, A., Menezes, I.F.M. (2010), "Polygonal finite elements for topology optimization: a unifying paradigm", *J. Numerical Methods Eng.,* **82**, 671–698. https://doi.org/ 10.1002/nme.2763.

Talischi, C., Paulino, G.H., Pereira, A., Menezes, I.F.M. (2012), "Polymesher: a general-purpose mesh generator for polygonal elements written in Matlab", *Struct. Multidisciplinary Opt.,***45**, 309–328. https://doi.org/ 10.1007/s00158-011-0706-z.

Ullah, Z., Augarde, C. (2013), "Finite deformation elasto-plastic modelling using an adaptive meshless method", *Comput. Struct.,***118**, 39–52. https://doi.org/ 10.1016/j.compstruc.2012.04.001.

Wachspress, E.L. (1975), *A Rational Finite Element Basis,* Academic Press, New York. https://doi.org/ 10.1115/1.3452953.

Wang, H., Qin, Q.H. (2017), "Voronoi polygonal hybrid finite elements with boundary integrals for plane isotropic elastic problems", *J. Appl. Mech.,* **9**, 1750031. https://doi.org/ 10.1142/S1758825117500314.

Warren, J. (1996), "Barycentric coordinates for convex polytopes", *Adv. Comput. Math.,* **6**, 97–108. https://doi.org/10.1007/BF02127699.

Zi, G., Rabczuk, T., Wolfgang W. (2007), "Extended meshfree methods without branch enrichment for cohesive cracks", *Comput. Mech.,* **40**, 367–382. https://doi.org/ 10.1007/s00466-006-0115-0.

Ziaei, H., Moslemi, H. (2020), "A new adaptive mesh refinement strategy based on a probabilistic error estimation", *Struct. Eng. Mech.*, **74**(4), 547-557. https://doi.org/10.12989/sem.2020.74.4.547.

Zienkiewicz, O.C., Zhu, J.Z. (1987), "A simple error estimator and adaptive procedure for practical engineering analysis", *J. Numerical Methods Eng.,* **24**, 337-357. https://doi.org/ 10.1002/nme.1620240206.

Zienkiewicz, O.C., Zhu, J.Z. (1992), "The superconvergent patch recovery (SPR) and adaptive finite element refinement", *Comput. Methods. Appl. Mech. Eng.,* **101**, 207-224. https://doi.org/ 10.1016/0045-7825(92)90023-D.

PL